Molecular Beam Epitaxy of $(Er_xSc_{1-x})_2O_3$ on Si(111) for Active Integrated Optical Devices

H. Omi[1,2], T. Tawara[1,2], T. Hozumi[3], R. Kaji[3], S. Adachi[3], H. Gotoh[1] and T. Sogawa[1]
[1]*NTT Basic Research Laboratories, NTT Corporation, Atsugi-shi, Japan*
[2]*NTT Nanophotonics Center, NTT Corporation, Atsugi-shi, Japan*
[3]*Hokkaido University, Sapporo, Japan*

Keywords: Er, Sc_2O_3, Si, Molecular Beam Epitaxy.

Abstract: We grew $(Er_xSc_{1-x})_2O_3$ films on Si(111) as a function of x using the molecular beam epitaxy method. The films were characterized by synchrotron grazing incidence and normal X-ray diffraction, cross-sectional transmission electron microscopy, and photoluminescence measurements in spectrum and time domains. We succeeded in obtaining $(Er_xSc_{1-x})_2O_3$ films on Si(111) that are strained and exhibit 1.5-μm light emission from Er^{3+} ions at 4 K and room temperature. We found that the epitaxial Er-doped Sc_2O_3 films are better candidates as a light emitting material than epitaxial layers of Er_2O_3 on Si(111).

SCIENCE AND TECHNOLOGY PUBLICATIONS

1 INTRODUCTION

Integration of cubic (bixbyite-type) sesquioxides on a Si platform has high potential to improve the performance of Si circuits by incorporating new functionalities as alternative gate oxides and light emitting materials (Grivas, 2008, Reiner, 2010, Bradley, 2011, Michael, 2009). Among the oxides, Sc_2O_3 is one of the most promising as a host material of rare-earth ions-doped light emitters on Si substrates (Grivas, 2008, Ter-Gabrielyan, 2011, Merkle, 2013). The thermal conductivity of Sc_2O_3 is the largest among the bixbyite-type oxides, including Y_2O_3 and rare earth oxides, and larger than that of yttrium aluminium garnet (YAG) crystal. The high thermal conductivity could enable us to obtain high-power light emission on Si. In fact, recent researches have shown that Er-doped Sc_2O_3 ceramics exhibit lasing at the wavelength of 1.58 μm with high quantum efficiency at low temperatures (Gheorghe, 2008, Kühn, 2009, Ter-Gabrielyan, 2011, Merkle, 2013). However, to the best of our knowledge, growth of Er-doped Sc_2O_3 has not been achieved on Si, even though Er ions have been successfully doped in Sc_2O_3 single and nano-crystals (Krsmanovic, 2006, Gün, 2007) and the energy levels of Er^{3+} in Sc_2O_3 ceramics are well-established (Trabelsi, 2010). This is mainly due to the large lattice misfit between Sc_2O_3 and Si. The misfit between lattice constant of Sc_2O_3 and two times that of Si is about 9%. Fortunately, despite the large misfit, high-quality Sc_2O_3 films with misfit dislocations have been grown on a miscut Si(111) as well as in the system of Gd_2O_3 on Si(111) by using the molecular beam epitaxy (MBE) method (Klenov, 2005, Hong, 2005, Chen, 2005). The defects, including such interfacial dislocations, however, should be avoided as much as possible for optical applications.

In this work, we grew epitaxial Er-doped Sc_2O_3 films on Si(111) using MBE as a function of Er concentration and characterized the structural and optical properties of the epitaxial films by synchrotron grazing incidence X-ray diffraction (GIXD), X-ray diffraction (XRD), cross-sectional transmission electron microscope (XTEM), and photoluminescence (PL) measurements. We will show that high-quality Er-doped epitaxial Sc_2O_3 films that exhibit 1.5-μm light emission from Er^{3+} ions can be grown on Si(111) by using MBE.

2 EXPERIMENTS

The heteroepitaxial growths of Er-doped Sc_2O_3 were performed on Si(111) substrates in an MBE chamber equipped with reflection high-energy diffraction (RHEED) apparatus. Sc_2O_3 and Er_2O_3 were

Omi H., Tawara T., Hozumi T., Kaji R., Adachi S., Gotoh H. and Sogawa T..
Molecular Beam Epitaxy of (ErxSc1-x)2O3 on Si(111) for Active Integrated Optical Devices.
DOI: 10.5220/0004762001750179
In *Proceedings of 2nd International Conference on Photonics, Optics and Laser Technology* (PHOTOPTICS-2014), pages 175-179
ISBN: 978-989-758-008-6
Copyright © 2014 SCITEPRESS (Science and Technology Publications, Lda.)

simultaneously deposited by electron beam depositions. The films were grown at the substrate temperature of 400 - 700℃. Before the depositions, a (7 × 7) structure was obtained on Si(111). Reflection high energy diffraction was used to monitor structures during the growth. Synchrotron GIXD experiments were performed at beamline BL15 in SPring-8. The incident X-ray energy was 15 keV. XRD measurements were also carried out in the single-crystal geometry using an X-ray diffraction diffractometer (X'pert-Pro MRD; Philips co.) with Cu K_α radiation. XTEM/X-ray energy dispersive spectroscopy (EDS) images were obtained at 300/200 kV. PL measurements were performed using a Raman/PL system (Renishaw, Model inVia Reflex/StreamLine). PL spectra were obtained at room temperature using a cooled InGaAs detector (Princeton Instruments, Model OMA-V:2.2). PL measurements at low temperatures were performed in another PL system (Omi, 2012, Tawara, 2013).

3 RESULTS AND DISCUSSION

Figure 1 shows the RHEED patterns obtained from the Si(111)-(7×7) surface and during the growth of $(Er_xSc_{1-x})_2O_3$ film on the Si(111)-(7×7) surface at 700℃. The RHEED pattern exhibits sharp streaks with a (4×4) structure, indicating that the epitaxial film grows two dimensionally on the Si(111) substrate. The formation of the (4×4) structure on the surface is in good accordance with the formation of Sc_2O_3 and Gd_2O_3 epitaxial layers on Si(111) (Trabelsi, 2010, Klenov, 2005, Hong, 2005, Wang, 2009).

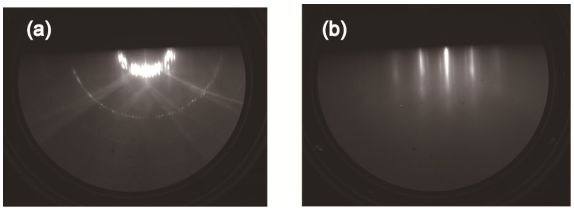

Figure 1: (a) (7 × 7) RHEED pattern from Si (111) substrate. (b) (4×4) RHEED pattern during $(Er_xSc_{1-x})_2O_3$ (x = 0.03) growth on Si(111). Electron beams are parallel to the <110> direction.

Figure 2 shows the θ–2θ scan XRD profile obtained from a 21-nm-thick $(Er_xSc_{1-x})_2O_3$ film grown on Si(111). The peaks at 2θ = 31.395 degrees is from the (222) reflections from the film. The relationship between the film and substrate is [111] $(Er_xSc_{1-x})_2O_3$//[111]Si. The lattice constant of the (222) plane is characterized to be 2.847 Å, which is between 2.843 Å for Sc_2O_3 and 3.045Å for Er_2O_3. The out-of-plane experiment shows that the lattice constant of the $(Er_xSc_{1-x})_2O_3$ film is almost equal to the lattice constant of Sc_2O_3. Additional ϕ scan experiments show that the film exhibits single domain on Si(111).

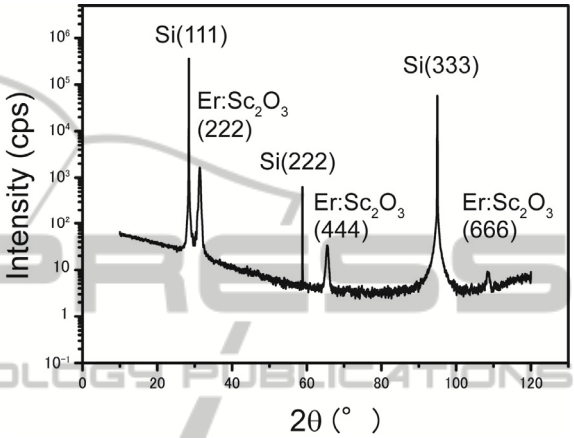

Figure 2: θ–2θ scan XRD profile obtained from the 21-nm-thick $(Er_xSc_{1-x})_2O_3$ (x = 0.03) film grown on Si(111).

Figure 3 shows the GIXD profile from the $(Er_xSc_{1-x})_2O_3$ film grown on Si(111). As seen in this figure, three peaks are evident in addition to the sharp peak from the Si(220). This suggests that the epitaxial film/Si(111) stacks have cube-on-cube structures with orientation relationships [111] $(Er_xSc_{1-x})_2O_3$//[111]Si and [1-10] $(Er_xSc_{1-x})_2O_3$//[-110]Si, which are consistent with those observed in the Sc_2O_3/Si(111) stacks (Chen, 2005). The main peak is from (440) reflection from the film, which is at 2θ = 12.452 degrees. From the peak position, the lattice constant of (440) is estimated to be 1.917Å, which almost matches the 1.92Å of Si(-220) planes, indicating that the epitaxial $(Er_xSc_{1-x})_2O_3$ films are significantly strained in-plane and that the lattice mismatch between Si and $(Er_xSc_{1-x})_2O_3$ film is not relieved by a hexagonal misfit dislocation networks, which were observed in the Sc_2O_3/Si(111) system by Klenov *et al.* (Klenov, 2005). Note here that the lattice constant of (440) planes are 1.74 and 1.865 Å for Sc_2O_3 and Er_2O_3, respectively. The peaks at 2θ = 12.071 and 13.008 degrees are from silicides formed at the interface between the film and substrate (See Fig. 4).

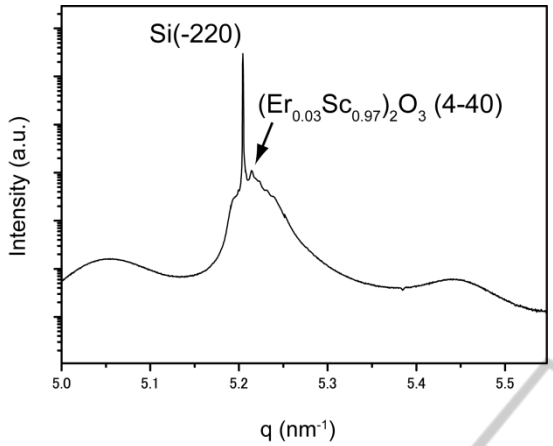

Figure 3: In-plane GIXD line scan around the $(Er_{0.03}Sc_{0.97})_2O_3$ (4-40) peak along [-110]Si.

Figure 4 shows an XTEM image obtained from the 21-nm-thick $(Er_xSc_{1-x})_2O_3$ film grown on Si(111). As seen in this image, we could not find significant defects in the film and oxide layers at the interface, indicating that we obtained high-quality epitaxial $(Er_xSc_{1-x})_2O_3$ layers on Si(111).

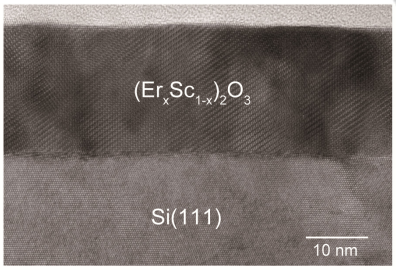

Figure 4: XTEM image of $(Er_{0.03}Sc_{0.97})_2O_3$ /Si(111).

Figure 5 shows an XTEM image and corresponding EDS images obtained from the $(Er_xSc_{1-x})_2O_3$ film grown on Si(111). The images clearly show that the $(Er_xSc_{1-x})_2O_3$ film coherently grows on Si(111). From the EDS mapping, we can see that the Er atoms are actually incorporated into the whole film and the Er concentration is estimated to be 1 at%. The Er concentration in the film was also confirmed to be 1.2 at% by an additional Rutherford back-scattering experiment. In addition, a nanoscale particle can be seen at the interface. Electron diffraction from the particle and EDS images show that the particle has the Sc_3Si_5 structure, which is in good agreement with the GIXD results in Fig 3.

Figure 6 shows the PL spectrum obtained at room temperature from the $(Er_xSc_{1-x})_2O_3$ films grown on Si(111) with pumping at 532 nm. The

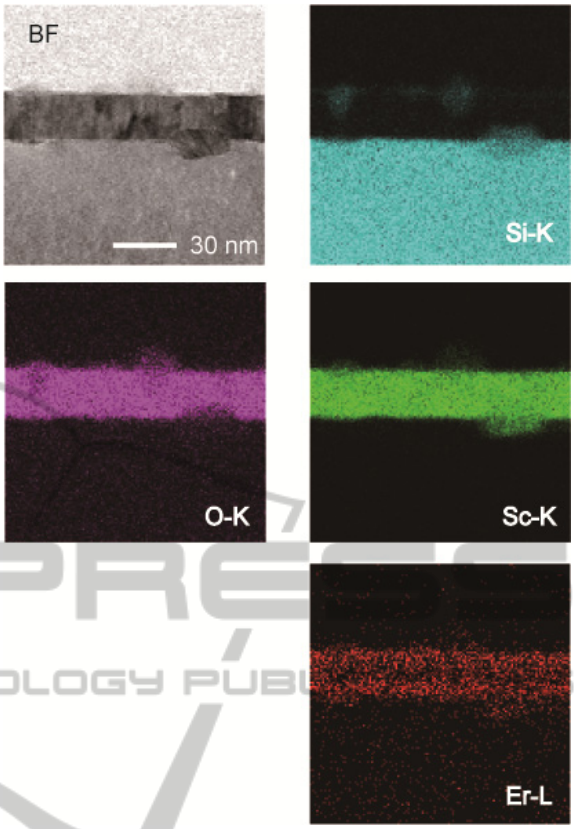

Figure 5: Bright field XTEM image (BF) and corresponding EDS images for Si, O, Sc, and Er.

films show PL emission at 1533 nm from Er^{3+} ions in the $(Er_xSc_{1-x})_2O_3$ films at x= 0.068, 0.134, and 0.676 and emission at 1535 nm in the Er_2O_3. The emissions are due to the transition between the energy levels ($^4I_{15/2}$ -$^4I_{13/2}$). The difference in the main peak positions indicates that the crystal fields around Er^{3+} ions in the $(Er_xSc_{1-x})_2O_3$ and Er_2O_3 are not identical. The peaks are observed to become broader with an increase of x, as seen in Fig. 7. We also obtained PL spectra from the films at 4 K with pumping at 1535 nm. The PL spectra have peaks at 1551 nm, which are originated from the transition between energy levels Y'_1 and Z'_1 of Er^{3+} ions located at C_{3i} sites of the $(Er_xSc_{1-x})_2O_3$ films with x = 0.068, 0.134, and 0.676 (Tawara, to be published). The peaks become sharper and their lifetime become longer (from the order of microseconds to milliseconds) than those of the epitaxial Er_2O_3 film grown on Si(111) by MBE at 4 K (Tawara, 2013).

For example, the lifetime of the 1.551-μm emission from Er^{3+} ions in the $(Er_{0.068}Sc_{0.932})_2O_3$ film was observed to be 2.2 ms at 4 K. The lifetime is compatible to those of $(Er_xYb_{1-x})_2SiO_5$ and $(Er_xY_{1-x})_2SiO_5$ polycrystalline films grown on Si substrates

when x is about 0.136 (Yin, 2012), indicating that the epitaxial layers have good potential as a optical-gain material.

Note that the interfacial silicides shown in Figs. 2 and 5 are optically inactive (Adler, 1992).

Finally, we discuss the quantum efficiency of Er^{3+} emission from the epitaxial $(Er_xSc_{1-x})_2O_3$ films on Si(111). For the films, the decay time τ of Er^{3+} emission is 150 μs at x = 1 (Tawara, 2013) and 2.2 ms at x = 0.068 (Tawara, to be submitted). The radiative life time τ_r of Er^{3+} in Y_2O_3 (Thiel, 2011) and SiO_2 (Lawrence 2013) are 14.6 and 20 ms, respectively. Therefore, quantum efficiency τ/τ_r is roughly estimated to be 1 % at x = 1 and on the order of 10 % at x = 0.068. We believe, however, that the quantum efficiency will become larger when x is optimized, as was observed in the polycrystalline $(Er_xY_{1-x})_2O_3$ films on Si(100) (Savio, 2009). Lifetime measurements of the epitaxial film as a function of x are in progress.

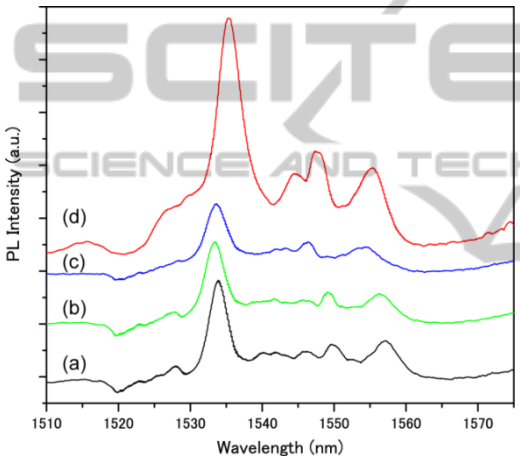

Figure 6: PL spectra obtained from the $(Er_xSc_{1-x})_2O_3$ films grown on Si(111) at room temperature with pumping at 532 nm. (a) x = 0.068, (b) x = 0.134, (c) x = 0.676, and (d) x = 1.

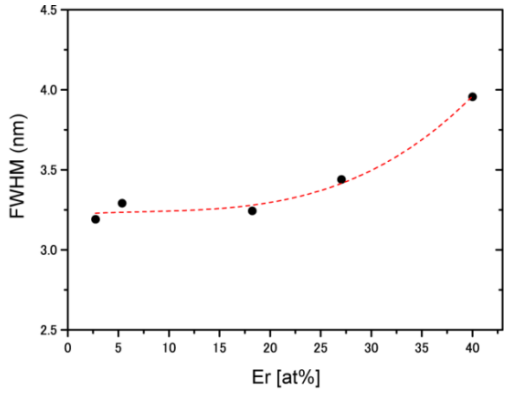

Figure 7: Plots of full width at half maximum (FWHM) of main peaks in Fig. 6 as a function of Er concentration in the epitaxial films. The FWHM of the main peaks are derived by fitting with Gaussian function. The dotted line is a guide for eye.

4 CONCLUSIONS

We succeeded in obtaining $(Er_xSc_{1-x})_2O_3$ epitaxial layers on Si(111) using the molecular beam epitaxy method with x from 0.068 to 1, even though they have large misfit between them. The as-grown film has a cubic bixbyite structure with three-fold symmetry. The films grew on Si(111) substrate with orientation relationships [111] $(Er_xSc_{1-x})_2O_3$//[111]Si and [1-10] $(Er_xSc_{1-x})_2O_3$//[-110]Si. The film at x = 0.068 is strained along the in-plane direction but not along the out-of-plane direction. The $(Er_xSc_{1-x})_2O_3$ films with x = 0.068, 0.134, and 0.676 exhibit PL luminescence at 1.5-μm at room temperature with pumping at 532 nm. The 1.551-μm luminescence becomes sharper and its lifetime becomes longer than those of Er_2O_3 epitaxial films on Si(111) at 4 K with pumping at 1535 nm. The Er-doped epitaxial Sc_2O_3 films have potential as an optical-gain material on the Si platform.

ACKNOWLEDGEMENTS

We thank Drs. Shingo Takeda and Kazushi Yokoyama for his help in the synchrotron radiation experiments at beamline BL15 in SPring-8. We also thank Prof. H. Isshiki and Dr. T. Nakajima for useful discussion. This work was partially supported by JSPS KAKENHI Grant Number 24360033.

REFERENCES

Adler D. L., Jacobson D. C., Eaglesham D. J., Marcus M. A., Benton J. L., Poate J. M., and Citrin P. H., 1992. *Appl. Phys. Lett.* 61, 2181.

Bradley J. D. B. and Pollnau, M. 2011. *Laser Photonics. Rev.* 5, 368.

Chen C. P., Hong M., Kwo J., Cheng H. M., Huang Y. L., Lin S. Y., Chi J., Lee H. Y., Hsieh Y. F., and Mannaerts J. P., 2005. *J. Crystal Growth* 278, 638.

Gheorghe C., Georgescu S., Lupei V., Lupei A., and Ikesue A., 2008. *J. Appl. Phys.* 103, 083116.

Gün T., Kuzminykh Y., Petermann K., Scheife H., and Huber G. 2007. *Appl. Phys. Lett.* 91, 083103.

Grivas C. and Eason R. W., 2008. *J. Phys.: Condens. Matter.* 20, 264011.

Hong M., Kortan A. R., Chang P., Huang Y. L., Chen C. P., and Chou H. Y., 2005. *Appl. Phys. Lett.* 87, 251902.
Klenov D. O., Edge L. F., Schlom D. G., and Stemmer S., 2005. *Appl. Phys. Lett.* 86, 051901.
Kühn H., Fechner M., Kahn A., Scheife H., and Huber G., 2009, *Opt. Mater*. 31, 1636.
Krsmanovic R., Lebedev O. I., Speghini A., Bettinelli M., Polizzi S., and Tendeloo G. V., 2006. *Nanotechnology* 17, 2805.
Lawrence N., Negro L. D., 2013. *Nano Lett*. 13, 3709.
Merkle L. D., Ter-Gabrielyan N., 2013. *Proc. SPIE* 8733, 87330H-8.
Michael C. P., Sabnis V. A., Yuen H. B., Jamora A., Semans S., Atanackovic P. B., and Painter O., 2009. *Appl. Phys. Lett.* 94, 131103.
Omi H. and Tawara T., 2012. *Jpn. J. Appl. Phys.* 51, 02BG07.
Reiner J. W., Kolpak A. M., Segal Y., Carrity K. F., Ismail-Beigi S., Ahn C. H., and Walker F., 2010. *Adv. Mater.* 22, 2919.
Savio R. L., Miritello M., Cardile P., Priolo F., 2009. *J. Appl. Phys.* 106, 043512.
Tawara T., Omi H., Hozumi T., Kaji R., Adachi S., Gotoh H., and Sogawa T., 2013. *Appl. Phys. Lett.* 102, 241918.
Tawara T., Omi H., Hozumi T., Kaji R., Adachi S., Gotoh H., and Sogawa T., *to be published.*
Ter-Gabrielyan N., Fromzel V., and Dubinskii M., 2011. *Opt. Mat. Expr.* 1, 503.
Thiel C. W., Böttger T., Cone R. L., 2011. *J. Lumin*. 131, 353.
Trabelsi I., Maalej R., Dammak M., Lupei A., and Kamoun M., 2010. *J. Lumin.*, 130, 927.
Wang J. X., Laha A., Fissel A., Schwendt D., Dargis R., Watahiki T., Shayduk R., Braun W., Liu T. M., and Osten H. J., 2009. *Semicond. Sci. Technol.* 24, 045021.
Yin L., Ning H., Turkdogan S., Liu Z., Nichols P., and Ning C. Z., 2012. *Appl. Phys. Lett.* 100, 241905.

SCITEPRESS
SCIENCE AND TECHNOLOGY PUBLICATIONS